

# Controlled Deposition Number of Organic Molecules Using Quartz Crystal Microbalance Evaluated by Scanning Tunneling Microscopy Single-Molecule-Counting

Eiichi Inami,<sup>\*,†,‡,§</sup> Masataka Yamaguchi,<sup>†</sup> Takayuki Yamaguchi,<sup>†</sup> Mikio Shimasaki,<sup>†</sup> and Toyo Kazu Yamada<sup>\*,†,§</sup>

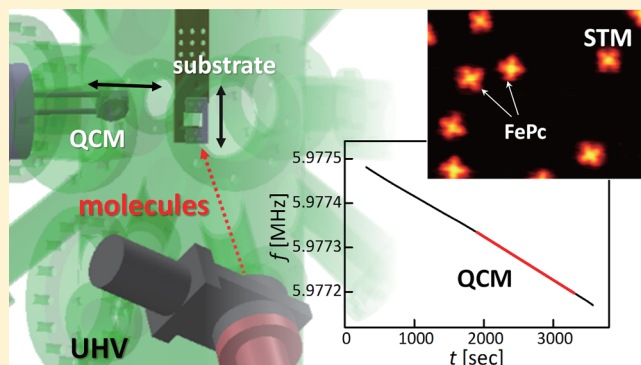
<sup>†</sup>Department of Materials Science, Chiba University, 1-33 Yayoi-cho, Inage-ku, Chiba 263-8522, Japan

<sup>‡</sup>School of Systems Engineering, Kochi University of Technology, 185 Miyanokuchi, Tosayamada, Kami, Kochi 782-8502, Japan

<sup>§</sup>Molecular Chirality Research Center, Chiba University, 1-33 Yayoi-cho, Inage-ku, Chiba 263-8522, Japan

## Supporting Information

**ABSTRACT:** Precise control of organic molecule deposition on a substrate is quite important for fabricating single-molecule-based devices. In this study, we demonstrate whether a quartz-crystal microbalance (QCM) widely used for a film growth calibration has the ability to precisely measure the number of organic molecules adsorbed on a substrate. The well-known Sauerbrey's equation is extended to formulate the relation between QCM resonant frequency shift and the number of adsorbed molecules onto the QCM surface. The formula is examined by QCM measurements of sublimation of  $\pi$ -conjugated organic molecules and direct counting of the deposited molecules one by one onto metal substrates, using ultrahigh vacuum low-temperature scanning tunneling microscopy (STM). It is revealed that the number of adsorbed molecules evaluated by QCM ( $N_{\text{QCM}}$ ) show good agreement with those counted from the STM images ( $N_{\text{STM}}$ ) within the error of  $\pm 25\%$ . The results ensure the QCM capability for controlling the deposition number of organic molecules with high accuracy, that is, if one needs to deposit 100 molecules on the substrate, QCM control promises deposition of  $100 \pm 25$  molecules.



A variety of organic molecular films supported by substrates have been used for molecular electronic devices, such as electroluminescence,<sup>1–5</sup> photovoltaic cells,<sup>6–12</sup> and field-effect transistor.<sup>13–15</sup> Some of these devices are realized by vacuum sublimation,<sup>3,4,6,11–13</sup> where the well-defined planar film with low defect/impurity concentration is grown on a substrate. In this method, a quartz-crystal microbalance (QCM) is used to control the thickness of the molecular films. QCM is a thickness-shear-mode acoustic wave mass-sensitive detector, where the attached foreign mass is observable through the shift in resonant frequency of the oscillating quartz crystal, as formulated by Sauerbrey.<sup>16</sup> To evaluate the film thickness from the measured mass change, the film density ( $\text{g}\cdot\text{cm}^{-3}$ ) is the one key parameter. For QCM measurement, the sublimated molecules are generally assumed to cover the whole acoustically active area of QCM surface, forming a uniform film with spatially constant density. This assumption is applicable if the film thickness is over a few tens of nanometers since the structure of such thick films is almost bulklike. Therefore, the film density can be calibrated by comparing the attached mass measured by QCM with the film thickness measured by the other techniques.<sup>17</sup>

On the other hand, recent extensive studies on single molecules on substrates<sup>18–25</sup> unveiled exciting novel properties that motivate us to fabricate high functional molecule-based devices.<sup>26,27</sup> To this end, the sophisticated regulation of the molecular deposition to prepare isolated single molecules or two-dimensionally ordered ultrathin molecular films (including monomolecular or a few molecular layers) on substrates is quite important. In such low coverage regions, however, the spatially constant film density cannot be assumed since the molecular aggregations are affected by the molecule–substrate interface and the bare film surface. Such a surface/interface causes the change in the separations of monomolecular layers depending on the layer number.<sup>25</sup> Further, under the submonolayer coverage regions, the molecules on substrate do not form films but exist as either islands (clusters) or single molecules, where the film density cannot be defined in principle. Therefore, thickness control is inadequate to precisely control deposition of small amounts of molecules.

Received: March 13, 2018

Accepted: June 27, 2018

Published: June 27, 2018

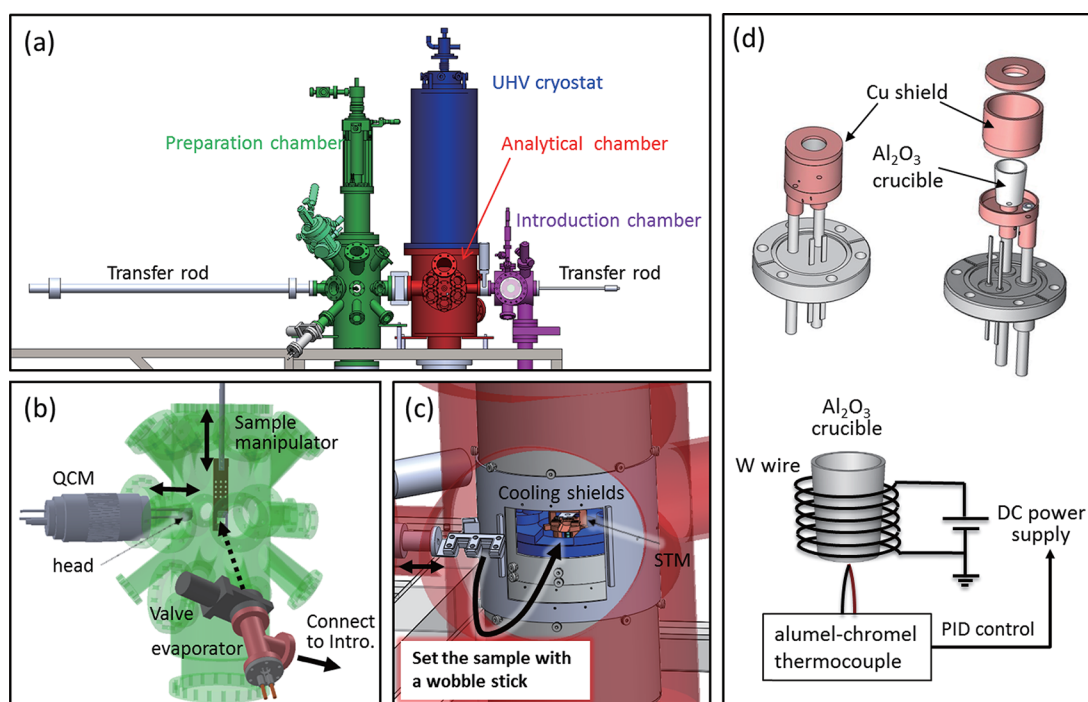


**Figure 1.** (a) Home-built UHV-LT-STM setup, consisting of three parts: introduction, preparation, and analytical chambers. Samples and tips were moved between these chambers with transfer rods. (b) Close-up view of the sample preparation chamber, where a quartz-crystal microbalance (QCM), a molecular evaporator, and a sample stage are shown. All point to the center of the chamber. (c) Close-up view of the analytical chamber, where the transfer rod, two cooling shields, and STM are shown. (d) Home-built molecular evaporator using a commercial UHV-ICF70 current feedthrough, where molecules in an  $\text{Al}_2\text{O}_3$  crucible were heated by flowing current through a W filament. An alumel–chromel thermocouple is located at the bottom of the crucible to measure the temperature of the crucible. Using the PID control power supply, the crucible temperature was stabilized during the evaporation.

Alternatively, the number of molecular depositions is important and should be varied in a controlled way.

In this article, we demonstrated control of the adsorption number of single organic molecules on the substrate by using QCM, whose accuracy was evaluated by direct counting of deposited molecules on the substrate one by one, using ultrahigh vacuum (UHV) low-temperature (LT) scanning tunneling microscopy (STM). Sauerbrey's equation<sup>16</sup> was extended to relate the number of adsorbed molecules onto the QCM plate with the resulting QCM frequency shift. The formula enabled us to control the number of adsorbed molecules on the substrate without information on the film density. The necessary information regarding the molecules was only the molar mass. That is, our method needed no preliminary calibration that is required for the conventional QCM measurement. The validity of our formula was examined by QCM measurements of sublimation of  $\pi$ -conjugated molecules [iron phthalocyanine (FePc) and metal-free tetraphenylporphine ( $\text{H}_2\text{TTP}$ )] and direct STM imaging of their depositions onto metal substrates [Cu(111) and Au(111)]. Markedly, the number of adsorbed single organic molecules controlled by QCM on the basis of our formula was in quite good agreement with that counted from the obtained STM image within an error of  $\pm 25\%$ .

## METHODS

The principle for measuring the number of adsorbed molecules by QCM is as follows. According to Sauerbrey,<sup>16</sup> mass changes at the QCM surface are generally expressed by

$$\Delta f = -\frac{2f_0^2}{(\mu_q \rho_q)^{1/2}} \Delta m = -C_m \Delta m \quad (1)$$

In this equation,  $\Delta f$  Hz is the measured frequency shift;  $f_0$  Hz is the resonant frequency of the quartz crystal;  $\Delta m$   $\text{g}\cdot\text{cm}^{-2}$  is the mass change per unit area at the QCM surface;  $\mu_q = 2.947 \times 10^{11} \text{ g}\cdot\text{cm}^{-1}\cdot\text{s}^{-2}$ , the shear modulus of quartz;  $\rho_q = 2.468 \text{ g}\cdot\text{cm}^{-3}$ , the density of quartz; and  $C_m = 8.15 \times 10^7 \text{ Hz}\cdot\text{g}^{-1}\cdot\text{cm}^2$ , the sensitivity factor. Under the assumption that the mass change is caused by the adsorptions of homogeneous molecules with the molar mass of  $M$ ,  $\Delta m$  can be expressed in terms of the number of adsorbed molecules per unit area  $n_{\text{QCM}} \text{ cm}^{-2}$  as  $\Delta m = Mn_{\text{QCM}}/N_A$ , where  $N_A = 6.02 \times 10^{23} \text{ mol}^{-1}$  is the Avogadro constant. Then, eq 1 can be rewritten as

$$\Delta f = -\frac{2f_0^2}{(\mu_q \rho_q)^{1/2}} \frac{M}{N_A} n_{\text{QCM}} = -C_n n_{\text{QCM}} \quad (2)$$

In this equation,  $C_n$  is the sensitivity factor. Note that eq 2 does not include the density of adsorbed molecules. Therefore, if we a priori know the  $M$  value of the target molecules,  $\Delta f$  can be directly converted to  $n_{\text{QCM}}$ . For example,  $f_0$  of the bare quartz in our system is 6 MHz (the sensitivity limit of  $\Delta f$  is 0.03 Hz). Therefore, if the  $M$  is assumed as  $600 \text{ g}\cdot\text{mol}^{-1}$ ,  $C_n$  is evaluated to be  $8 \times 10^{-14} \text{ Hz}\cdot\text{cm}^2$ . In this condition,  $n_{\text{QCM}} = -\Delta f/C_n$  (see eq 2) means that the QCM could have an ability to detect one organic molecule adsorption per  $17 \times 17 \text{ nm}^2$  area.

## EXPERIMENTAL SECTION

All experiments were performed using a home-built UHV-LT-STM setup (base pressure  $<8 \times 10^{-9}$  Pa). Our system comprises an introduction, a preparation, and an STM analytical chamber (see Figure 1a), which are interconnected for performing substrate cleaning, molecular deposition, and STM observation without exposing the sample to the atmosphere.

**Sample Preparations.** Cu(111) and Au(111) were used as substrates. Both substrates were subjected to several cycles of Ar<sup>+</sup> ion sputtering (1 kV) and annealing [873 K for Cu(111), and 800 K for Au(111)] in the preparation chamber, by which cleaned and atomically flat surfaces were obtained. As test molecules, two types of  $\pi$ -conjugated molecules, FePc and H<sub>2</sub>TPP, were used. FePc powder (Aldrich, purity 90%) was purified by sublimation at 653 K and by recrystallization at 453 K under the pressure of  $10^{-1}$  Pa (yield 12%), while the purification was not performed for H<sub>2</sub>TPP powder. The molecular powders were then placed into the Al<sub>2</sub>O<sub>3</sub> crucible in a home-built molecular evaporator and were pumped down to  $10^{-8}$  Pa.

**Molecular Evaporator.** As shown in Figure 1b, the evaporator was set at one of the ports in the preparation chamber pointing toward the center of the chamber. A gate valve was used as a shutter to separate the evaporator and the preparation chamber. The evaporator was also connected to the introduction chamber for exchanging the molecule without breaking the UHV of the preparation chamber. Figure 1d shows the sketch of the evaporator. A W wire (diameter 0.3 mm) was set around the crucible, which was used as a filament by flowing current (0–6 A). An alumel–chromel thermocouple was located at the bottom of the crucible. The crucible and the filament were shielded by a Cu cylinder to make a crucible temperature equivalent. Using a proportional-integral-derivative (PID) controller of the power supply, the crucible temperature during the molecular evaporation could be precisely controlled (see Supporting Information).

**Molecular Deposition.** Prior to molecular depositions, the deposition rates were first monitored by QCM (Inficon, 6 MHz, 14 mm diameter, AT-cut quartz crystal with Au electrode) in the preparation chamber (see Figure 1b). During the measurement, the QCM head was placed at the center of the preparation chamber. After setting the crucible temperature at predetermined values, the QCM resonant frequency  $f$  was measured with the gate valve opened. Following the QCM measurement, the QCM head was withdrawn, and the substrate was alternatively placed at the center of the preparation chamber to start molecular depositions. During the deposition, the pressure in the preparation chamber was about  $10^{-8}$ – $10^{-7}$  Pa. After molecular depositions, the sample was quickly set to the STM stage located in the analytical chamber which was cooled by a UHV-cryostat. Surrounding the STM, 5 and 80 K cooling shields cut heat radiation. The sample in the STM stage could be quickly exchanged by opening doors on the shields with a wobble stick (see Figure 1c).

**Sample Characterization.** STM measurements were performed in the constant current mode at 4.7 K with liquid-He and at 78 K with liquid-N<sub>2</sub>. Electrochemically etched W-tips ( $\phi = 0.3$  mm, purity 99.99%) were used for the STM probe. Each tip was carefully cleaned by annealing in the

introduction chamber<sup>28</sup> and then subsequently setting into the STM stage.

## RESULTS AND DISCUSSION

**Deposition of Submonolayer FePc on Cu(111).** To check the earlier idea, we compared the number of adsorbed molecules on substrates between QCM and STM measurement (see the Experimental Section). Figure 2a shows the time

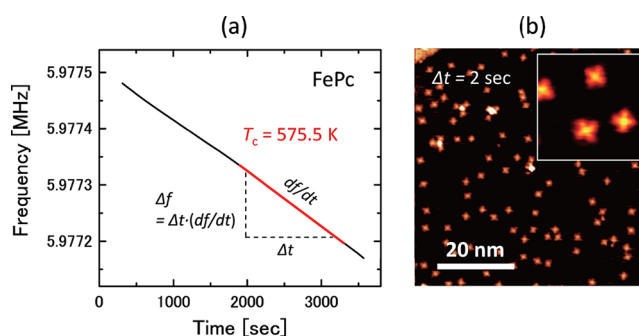


**Figure 2.** (a) QCM resonant frequency as a function of time during sublimation of FePc molecules. The red line is a linear fit at constant crucible temperature of 575.5 K. (b) STM topography image (at 4.7 K) of Cu(111) surface after FePc deposition with the crucible temperature of 575.5 K for 2 s ( $60 \times 60$  nm<sup>2</sup>,  $-0.5$  V, 200 pA). The inset is the magnified view, focusing on the single FePc molecules.

dependence of  $f$  during sublimation of FePc molecules ( $M = 568.38$  g·mol<sup>-1</sup>). The crucible temperature ( $T_c$ ) is gradually increased and is kept at 575.5 K. At the constant  $T_c$ , the  $f$  decreases linearly with time (red line in Figure 2a). From the slope ( $df/dt = -9.82 \times 10^{-2}$  Hz·s<sup>-1</sup>),  $\Delta f$  can be simply obtained by setting the deposition time  $\Delta t$  as  $\Delta f = \Delta t \cdot (df/dt)$ , and thus, the corresponding  $n_{\text{QCM}}$  value can also be obtained by  $n_{\text{QCM}} = -\Delta f/C_n$  (see eq 2).

At this crucible temperature (575.5 K), the molecules were deposited on Cu(111) surface, and then, the surface was imaged by STM. The  $\Delta t$  was set at 2 s, from which  $\Delta f [= \Delta t \cdot (df/dt)]$  was obtained as  $-0.1964$  Hz. Therefore, the corresponding  $n_{\text{QCM}} (= -\Delta f/C_n)$  was obtained as  $2.55 \times 10^{-2}$  nm<sup>-2</sup> (see Table 1 for the other parameters). Figure 2b is the resulting STM image. The FePc molecules were adsorbed on the bare Cu(111) surfaces as single molecules each of which appears as four-lobed shaped with a center brighter spot (inset of Figure 2b). From the image, the number of adsorbed molecules per the STM image area ( $60 \times 60$  nm<sup>2</sup>) was counted to be  $N_{\text{STM}} = 123$ , while  $N_{\text{QCM}}$  ( $n_{\text{QCM}} \times \text{STM image area}$ ) was evaluated as 91.9 (see Table 1). Namely, the obtained  $N_{\text{STM}}$  and  $N_{\text{QCM}}$  showed not perfect, but rather under control with an error [ $100 \cdot (N_{\text{QCM}} - N_{\text{STM}})/N_{\text{STM}}$ ] of about  $-25\%$ .

**Deposition of 1 ML FePc on Cu(111).** We also examined the QCM capability in the higher coverage region. Experimentally, FePc molecules were deposited on Cu(111) surface with  $T_c = 581.0$  K for 20 s. Therefore, in a similar manner as in Figure 2a, the  $df/dt$  can be obtained by linear fit as  $-1.26 \times 10^{-1}$  Hz·s<sup>-1</sup> (red line in Figure 3a). Subsequently, the corresponding  $\Delta f [= \Delta t \cdot (df/dt)]$  and  $n_{\text{QCM}} (= -\Delta f/C_n)$  were also obtained to be  $-2.52$  Hz and  $3.27 \times 10^{-1}$  nm<sup>-2</sup>, respectively (see Table 1). Here, the obtained  $n_{\text{QCM}}$  value indicates that the space where the single molecule can occupy ( $1/n_{\text{QCM}} = 1.75 \times 1.75$  nm<sup>2</sup>) is almost comparable with the

Table 1. Summary of the QCM and STM Experimental Results<sup>a</sup>

	$M$ [g·mol <sup>-1</sup> ]	$C_n$ [Hz·cm <sup>2</sup> ]	$T_c$ [K]	$\Delta t$ [s]	$df/dt$ [Hz·s <sup>-1</sup> ]	$\Delta f$ [Hz]	$n_{\text{QCM}}$ [nm <sup>-2</sup> ]	$N_{\text{QCM}}$ [/image]	$N_{\text{STM}}$ [/image]	error [%]
FePc/Cu(111)	568.38	$7.70 \times 10^{-14}$	575.5	2	$-9.82 \times 10^{-2}$	-0.196	$2.55 \times 10^{-2}$	91.9	123	-25
			581	20	$-1.26 \times 10^{-1}$	-2.520	$3.27 \times 10^{-1}$	818.7	913	-10
H <sub>2</sub> TPP/Au(111)	614.74	$8.32 \times 10^{-14}$	416.4	40	$-1.74 \times 10^{-2}$	-0.696	$8.36 \times 10^{-2}$	301.0	271	11
			416.4	300	$-1.87 \times 10^{-2}$	-5.610	$6.74 \times 10^{-1}$	2591.0	2875	-10

<sup>a</sup> $M$  is the molar mass,  $C_n$  is the sensitivity factor,  $T_c$  is the crucible temperature,  $\Delta t$  is the deposition time,  $df/dt$  is the changing rate of the QCM resonant frequency,  $\Delta f$  is the change of the QCM resonant frequency,  $n_{\text{QCM}}$  is the number of adsorbed molecules per unit area,  $N_{\text{QCM}}$  is the number of adsorbed molecules per an STM image evaluated by QCM, and  $N_{\text{STM}}$  is the number of adsorbed molecules counted from an STM image. Error was evaluated from  $100 \cdot (N_{\text{QCM}} - N_{\text{STM}}) / N_{\text{STM}}$ .

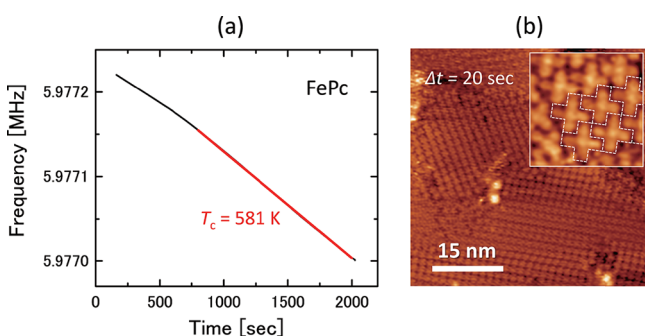


**Figure 3.** (a) QCM resonant frequency as a function of time during sublimation of FePc molecules. The red line is a linear fit at constant crucible temperature of 581.0 K. (b) STM topography image (at 4.7 K) of Cu(111) surface after FePc deposition with the crucible temperature of 581.0 K for 20 s ( $50 \times 50 \text{ nm}^2$ , 1.0 V, 50 pA). The inset is the magnified view, focusing on the single FePc molecules.

size of single FePc ( $1.5 \times 1.5 \text{ nm}^2$ ). This means that the molecular coverage is around 1 ML. Indeed, the resulting STM image (Figure 3b) reveals that the Cu(111) surface with  $50 \times 50 \text{ nm}^2$  area is fully covered with the well-ordered FePc films. From the image, the  $N_{\text{STM}}$  is counted to be 913, while  $N_{\text{QCM}}$  is 818.7 (see Table 1), showing again not perfect but rather good agreement with an error  $[100 \cdot (N_{\text{QCM}} - N_{\text{STM}}) / N_{\text{STM}}]$  of -11%.

**Deposition of H<sub>2</sub>TPP on Au(111).** To further verify the reliability of the QCM capability, the same experiments were performed using a different molecule–substrate system. As the molecule, H<sub>2</sub>TPP ( $M = 614.74 \text{ g} \cdot \text{mol}^{-1}$ ) was sublimated, and Au(111) was used as the substrate. Figure 4 shows the two sets of experiments (labeled EXP. I and EXP. II). Since the  $T_c$  for both experiments was set at 416.4 K, the slopes of the  $f$  (red and blue lines in Figure 4a) showed similar values ( $df/dt = -1.74 \times 10^{-2} \text{ Hz} \cdot \text{s}^{-1}$  for EXP. I, and  $df/dt = -1.87 \times 10^{-2} \text{ Hz} \cdot \text{s}^{-1}$  for EXP. II). The slight difference in  $df/dt$  values at the same  $T_c$  comes from the experimental error (the details are discussed later). Meanwhile, to change the molecular coverages, the  $\Delta t$  values were set at 40 s for EXP. I and at 300 s for EXP. II. Then, the  $n_{\text{QCM}}$  ( $= -\Delta f / C_n$ ) was obtained to be  $8.36 \times 10^{-2} \text{ nm}^{-2}$  for EXP. I and  $6.74 \times 10^{-1} \text{ nm}^{-2}$  for EXP. II (see Table 1 for the other parameters). Because the molecular size of single H<sub>2</sub>TPP is about  $1.6 \times 1.6 \text{ nm}^2$ , the coverages ( $n_{\text{QCM}}$  molecular size) were roughly estimated as 0.21 ML for EXP. I and 1.73 ML for EXP. II.

In this case, the coverage expectations were also reasonable with the resulting STM images (Figure 4b and c), that is, the H<sub>2</sub>TPP appeared as single molecules on bare Au(111) surface for EXP. I (Figure 4b), while the whole surface was covered with H<sub>2</sub>TPP for EXP. II (Figure 4c). Similar to the case in

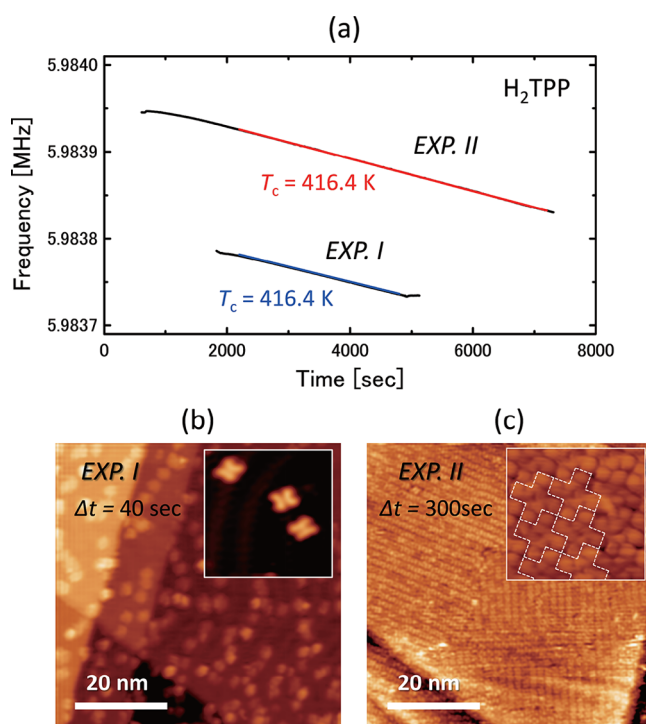


**Figure 4.** (a) Two sets of QCM resonant frequency as a function of time during sublimation of H<sub>2</sub>TPP molecules. Red and blue lines are linear fits at constant crucible temperature of 416.4 K. (b, c) STM topography images (at 78 K) of Au(111) surface after H<sub>2</sub>TPP deposition for (b) 40 s ( $60 \times 60 \text{ nm}^2$ , -1.0 V, 50 pA) and (c) 300 s ( $62 \times 62 \text{ nm}^2$ , -1.5 V, 20 pA). The crucible temperature is 416.4 K. The insets in b and c are the magnified views, focusing on the single molecules.

FePc/Cu(111), the  $N_{\text{STM}}$  for both experiments was obtained from the STM images to be  $N_{\text{STM}} = 271$  for EXP. I and  $N_{\text{STM}} = 2875$  for EXP. II. Here, we note that the  $N_{\text{STM}}$  for EXP. II was obtained by doubling the number of H<sub>2</sub>TPP molecules counted from the STM image (Figure 4c) since the coverage estimated from  $n_{\text{QCM}}$  was around 2 ML. Remarkably, these  $N_{\text{STM}}$  values also showed good correspondence with  $N_{\text{QCM}} = 301$  for EXP. I and  $N_{\text{QCM}} = 2591$  for EXP. II (see Table 1), that is, these errors  $[100 \cdot (N_{\text{QCM}} - N_{\text{STM}}) / N_{\text{STM}}]$  were 11% and -10%, respectively.

**Accuracy of QCM Measurements.** Table 1 summarizes our results of QCM and STM measurements. The obtained  $N_{\text{QCM}}$  and  $N_{\text{STM}}$  are not perfectly fit with an accuracy of one single molecule, but the numbers are rather good agreements within an error of  $\pm 25\%$ , indicating high reliability of the present method. The slight errors less than 25% can be attributed to the following reasons. First, since the QCM plate

has not been subjected to any cleaning procedures, the surface should be topographically rough and covered by unknown impurities, which is clearly different from atomically flat/clean metal substrates [Cu(111) and Au(111)]. Correspondingly, the molecular adsorption rates should also be different between the QCM surface and the metal substrates. In the case of the thick molecular film, this effect is negligible since a large fraction of molecules are absorbed mostly onto the pre-existing molecules. However, in the case of deposition of a small amount of molecules, such different adsorption rates affect the number of adsorbed molecules, which may cause the deviation of  $N_{\text{QCM}}$  from  $N_{\text{STM}}$ . Because of this factor, the adsorption rate of the QCM surface also fluctuates in each measurement since the atomic-scale surface morphology is not perfectly the same. We consider that this could cause the non-negligible experimental error, such as different  $df/dt$  values obtained even at the same  $T_c$  (see Table 1). Direct STM imaging of the QCM surface before/after molecular sublimation and comparing the QCM measurement will provide us useful information on this factor, which is one interesting future work. Second, as mentioned earlier, Sauerbrey's equation (eq 1) assumes that the sublimated molecules cover the whole surface of the QCM plate as a uniform film, while sublimation of a small amount of molecules results in the adsorptions as isolated single molecules and spatially inhomogeneous molecular film. Since the sensitivity of the frequency response to a mass deposited is not constant but depends on the positions on the plate (the sensitivity decreases with the radial distance from the center of the QCM surface),<sup>29,30</sup> application of eq 1 to the present experiment may cause the slight deviation of  $N_{\text{QCM}}$  from the actual value. For example, as the simple case, we assume that two molecules are adsorbed on the QCM plate; one is adsorbed at the center of the plate and another is at the plate edge. In this case, QCM is sensitive to the former molecule while slightly insensitive to the latter one. Consequently,  $N_{\text{QCM}}$  will be smaller than the actual value ( $N_{\text{QCM}} = 2$ ). Third, Sauerbrey's equation (eq 1) also assumes that the acoustic impedance (defined as the square root of the product of the density and shear modulus of the film) is identical to that of quartz crystal.<sup>16,30</sup> In the present experiment, however, the density and the shear modulus of the molecules are unknown parameters; thereby, the validity of the assumption of eq 1 cannot be confirmed. If the acoustic impedances of the film deviate from that of quartz crystal, reflections of the acoustic wave at the interface disturb the reliability of eq 1. Nevertheless, our experiment demonstrates that such ambiguous factors cause only slight errors ( $\leq 25\%$ ), thereby not so critical that hamper the precise QCM measurements.

## CONCLUSIONS

In conclusion, accuracy of the number of adsorbed organic molecules (FePc and  $\text{H}_2\text{TPP}$ ) controlled by QCM was evaluated by direct counting of molecules one by one using STM. We found that the number has an error of  $\pm 25\%$ , that is, if one needs to deposit 100 molecules, QCM promises an accuracy of deposition of  $100 \pm 25$  molecules on the substrate. This conclusion remains regardless of the morphologies of the adsorbed molecules on the substrates. Moreover, although the present study focused on deposition of pure molecules, the method can also be applicable for codepositions of different molecules and, thus, can be utilizable in a wide range of fields. The present method requires no additional experimental setup

to the conventional QCM system and, thus, possibly becomes a standard technique for sophisticated regulations of the molecular depositions toward high functional molecule-based devices.

## ASSOCIATED CONTENT

### Supporting Information

The Supporting Information is available free of charge on the ACS Publications website at DOI: 10.1021/acs.analchem.8b01118.

Controllability of a crucible temperature during molecular evaporation by use of PID controlled power supply (PDF)

## AUTHOR INFORMATION

### Corresponding Authors

\*E-mail: inami.eiichi@kochi-tech.ac.jp.

\*E-mail: toyoyamada@faculty.chiba-u.jp.

### ORCID

Eiichi Inami: 0000-0002-2167-8510

### Notes

The authors declare no competing financial interest.

## ACKNOWLEDGMENTS

We thank professor Hideki Yorimitsu (Kyoto University) for providing the sample of  $\text{H}_2\text{TPP}$ . This work was supported by JSPS KAKENHI Grant Number (16K17521, 16K05887, JP25110011, 17H05353). One of the authors (E. I.) also acknowledges financial support from the Murata Science Foundation.

## REFERENCES

- (1) Tang, C. W.; VanSlyke, S. A.; Chen, C. *J. Appl. Phys.* **1989**, *65*, 3610–3616.
- (2) Coe, S.; Woo, W.-K.; Bawendi, M.; Bulovic, V. *Nature* **2002**, *420*, 800.
- (3) Van Slyke, S. A.; Chen, C.; Tang, C. W. *Appl. Phys. Lett.* **1996**, *69*, 2160–2162.
- (4) Kaji, H.; Suzuki, H.; Fukushima, T.; Shizu, K.; Suzuki, K.; Kubo, S.; Komino, T.; Oiwa, H.; Suzuki, F.; Wakamiya, A.; Murata, Y.; Adachi, C. *Nat. Commun.* **2015**, *6*, 8476.
- (5) Tan, Z.-K.; Moghaddam, R. S.; Lai, M. L.; Docampo, P.; Higler, R.; Deschler, F.; Price, M.; Sadhanala, A.; Pazos, L. M.; Credgington, D.; Hanusch, F.; Bein, T.; Snaith, H. J.; Friend, R. H. *Nat. Nanotechnol.* **2014**, *9*, 687–692.
- (6) Zhao, J.; Li, Y.; Yang, G.; Jiang, K.; Lin, H.; Ade, H.; Ma, W.; Yan, H. *Nat. Energy* **2016**, *1*, 15027.
- (7) Tang, C. W. *Appl. Phys. Lett.* **1986**, *48*, 183–185.
- (8) Burschka, J.; Pellet, N.; Moon, S.-J.; Humphry-Baker, R.; Gao, P.; Nazeeruddin, M. K.; Grätzel, M. *Nature* **2013**, *499*, 316–319.
- (9) Jeon, N. J.; Noh, J. H.; Kim, Y. C.; Yang, W. S.; Ryu, S.; Seok, S. I. *Nat. Mater.* **2014**, *13*, 897–903.
- (10) Jeon, N. J.; Noh, J. H.; Yang, W. S.; Kim, Y. C.; Ryu, S.; Seo, J.; Seok, S. I. *Nature* **2015**, *517*, 476–480.
- (11) Liu, M.; Johnston, M. B.; Snaith, H. J. *Nature* **2013**, *501*, 395–398.
- (12) Chen, Q.; Zhou, H.; Hong, Z.; Luo, S.; Duan, H.-S.; Wang, H.-H.; Liu, Y.; Li, G.; Yang, Y. *J. Am. Chem. Soc.* **2014**, *136*, 622–625.
- (13) Kraus, M.; Richler, S.; Opitz, A.; Brutting, W.; Haas, S.; Hasegawa, T.; Hinderhofer, A.; Schreiber, F. *J. Appl. Phys.* **2010**, *107*, 094503.
- (14) Zielke, D.; Hübler, A. C.; Hahn, U.; Brandt, N.; Bartzsch, M.; Fügmann, U.; Fischer, T.; Veres, J.; Ogier, S. *Appl. Phys. Lett.* **2005**, *87*, 123508.

- (15) Mei, Y.; Loth, M. A.; Payne, M.; Zhang, W.; Smith, J.; Day, C. S.; Parkin, S. R.; Heeney, M.; McCulloch, I.; Anthopoulos, T. D.; Anthony, J. E.; Jurchescu, O. D. *Adv. Mater.* **2013**, *25*, 4352–4357.
- (16) Sauerbrey, G. *Eur. Phys. J. A* **1959**, *155*, 206.
- (17) Lindner, M.; Schmid, M. *Coatings* **2017**, *7*, 9.
- (18) Auwärter, W.; Seufert, K.; Bischoff, F.; Eciija, D.; Vijayaraghavan, S.; Joshi, S.; Klappenberger, F.; Samudrala, N.; Barth, J. V. *Nat. Nanotechnol.* **2012**, *7*, 41–46.
- (19) Perera, U. G. E.; Ample, F.; Kersell, H.; Zhang, Y.; Vives, G.; Echeverria, J.; Grisolia, M.; Rapenne, G.; Joachim, C.; Hla, S.-W. *Nat. Nanotechnol.* **2013**, *8*, 46–51.
- (20) Schmaus, S.; Bagrets, A.; Nahas, Y.; Yamada, T. K.; Bork, A.; Bowen, M.; Beaurepaire, E.; Evers, F.; Wulfhekel, W. *Nat. Nanotechnol.* **2011**, *6*, 185–189.
- (21) Kawahara, S. L.; Lagoute, J.; Repain, V.; Chacon, C.; Girard, Y.; Rousset, S.; Smogunov, A.; Barreteau, C. *Nano Lett.* **2012**, *12*, 4558–4563.
- (22) Bagrets, A.; Schmaus, S.; Jaafar, A.; Kramczynski, D.; Yamada, T. K.; Alouani, M.; Wulfhekel, W.; Evers, F. *Nano Lett.* **2012**, *12*, 5131–5136.
- (23) Schuler, B.; Fatayer, S.; Mohn, F.; Moll, N.; Pavliček, N.; Meyer, G.; Peña, D.; Gross, L. *Nat. Chem.* **2016**, *8*, 220–224.
- (24) Yamada, T. K.; Yamagishi, Y.; Nakashima, S.; Kitaoka, Y.; Nakamura, K. *Phys. Rev. B: Condens. Matter Mater. Phys.* **2016**, *94*, 195437.
- (25) Inami, E.; Shimasaki, M.; Yorimitsu, H.; Yamada, T. K. *Sci. Rep.* **2018**, *8*, 353.
- (26) Joachim, C.; Gimzewski, J. K.; Aviram, A. *Nature* **2000**, *408*, 541–548.
- (27) Barth, J. V.; Costantini, G.; Kern, K. *Nature* **2005**, *437*, 671–679.
- (28) Yamada, T. K.; Abe, T.; Nazriq, N. M. K.; Irisawa, T. *Rev. Sci. Instrum.* **2016**, *87*, 033703.
- (29) Ward, M. D.; Delawski, E. J. *Anal. Chem.* **1991**, *63*, 886–890.
- (30) Buttry, D. A.; Ward, M. D. *Chem. Rev.* **1992**, *92*, 1355–1379.